

Simulation Study of Kurtosis Measurements in MR Diffusion Kurtosis Imaging

K. H. Cheng^{1,2}, and E. X. Wu^{2,3}

¹Medical Engineering Programme, The University of Hong Kong, Pokfulam, Hong Kong, ²Laboratory of Biomedical Imaging and Signal Processing, The University of Hong Kong, Pokfulam, Hong Kong, ³Department of Electrical & Electronic Engineering, The University of Hong Kong, Pokfulam, Hong Kong

INTRODUCTION

Use of MRI to investigate the complex neural tissue structures has long been a vigorous research topic for years. Various parameters have been evaluated to characterize the tissue microstructures and their pathological alterations in brain and spinal cord. The insufficiency of the conventional diffusion weighted imaging (DWI) was supplemented by diffusion tensor imaging (DTI) through the analysis of axial and radial diffusivities. However, even DTI does not fully utilize the information from MR diffusion measurement with regard to the cellular structure. Generalized diffusion tensor imaging (GDTI) (1,2) has been formulated in attempt to obtain more information. Diffusion kurtosis imaging (DKI), a relatively more feasible imaging modality than q-space imaging, has been recently proposed and demonstrated for tissue characterization (3-7). Apparent diffusion kurtosis is obtained by using multiple b-value measurements to fit a signal attenuation equation $\ln(S/S_0) = -bD_{app} + b^2 D_{app}^2 K_{app}/6 + O(b^3)$, which is equivalent to the GDTI approach truncated to the 2nd order. Diffusion coefficient is defined mathematically as $\langle s^2 \rangle / (2t)$ and kurtosis $(\langle s^4 \rangle / \langle s^2 \rangle^2) - 3$ where s is the displacement and t is the diffusion time. The objective of this simulation study is to evaluate the adequacy of DKI in estimating diffusion kurtosis and assessing the restricted diffusion environment.

METHOD

Monte Carlo simulation was performed in 1D space to study the spin diffusion, kurtosis characteristics, spin dephasing and MR signal attenuation for various diffusion and MR parameters. Restricted diffusion was achieved by placing partially permeable barriers (permeability = 0.01 $\mu\text{m}/\text{ms}$) in between 100,000 spins initially evenly distributed and with barrier passing probability given in (8). If a spin could not pass through the barrier, it would bounce back. Each diffusion step-distance was randomly generated with variance equal to $2D(dt)$, where D was taken as the intrinsic diffusion coefficient of water ($2.2 \mu\text{m}^2/\text{ms}^{-1}$) and dt the step time. The phase accumulation and the rephasing during the initial and final pulses in PGSE were calculated with each diffusion step (9). The simulated signal attenuation was computed by $S = S_0 \langle e^{i\phi} \rangle$ where ϕ was the phase accumulated by each spin. The apparent kurtosis K_{app} and apparent diffusion coefficient were then estimated by fitting to the signal attenuation equation above (truncated GDTI for DKI), and compared to the true kurtosis and diffusion coefficient calculated from the actual diffusion displacement profiles. All simulations are performed with a range of b values with maximum b of $6\text{ms}/\mu\text{m}^2$.

RESULTS

The algorithm was first tested for free diffusion (Fig.1), in which case the signal attenuation followed the mono-exponential trend. For restricted water diffusion with compartmental partition sizes of $7 \mu\text{m}$ (Case A) and diffusion times ranging from 30 ms to 230 ms, the fitted or apparent kurtosis K_{app} was found to consistently overestimate the true kurtosis (Fig.2). At long diffusion times, the difference between K_{app} and true kurtosis became less. The curves also show a characteristic peak region at diffusion time around 50 ms. With compartmental partition sizes of $13 \mu\text{m}$ (Case B), the corresponding curves show a similar trend as in Case A, however, with less discrepancy between apparent and true kurtosis and the peak location shifted toward the long diffusion time (Fig.3).

DISCUSSIONS

The simple 1D simulations here demonstrate the presence of discrepancies when using apparent kurtosis to represent the true diffusion kurtosis. The results show that kurtosis in compartment-restricted diffusion is revealed effectively by DKI only when the optimal diffusion time, gradient and b value range are chosen. In simulation Case A, K_{app} follows the same trend as the true kurtosis. In particular, sufficient diffusion time is required for the spins to encounter the barriers and thus probe the restrictive barriers. More importantly, both apparent and true diffusion kurtosis also depend on the diffusion within individual compartments, diffusion time, and structural dimensions of restricted diffusion environment. For example, the diffusion displacement profiles shown in Fig. 4 illustrate the effect of diffusion time on diffusion kurtosis (in Case A, i.e., partition size of $7 \mu\text{m}$). As diffusion time increases, the diffusion profile becomes smoother, suggesting that the spins start to "overcome" the barriers. Similar trend was also observed in our in vivo measurement of apparent radial kurtosis (perpendicular to the axonal direction) in adult rat brain white matter tissues (corpus callosum - CC; external capsule - EC; cerebral peduncle - CP; anterior commissure - AC) at 7 T with six b values ranging from 0 to $2.5 \text{ms}/\mu\text{m}^2$ (Fig. 5).

CONCLUSIONS

Although DKI formulation provides an efficient way to probe the diffusion restriction by examining water diffusion information on higher order, the simulations here show that errors can be present in estimating true diffusion kurtosis by the apparent kurtosis obtained from DKI experiments. Choices of diffusion weighting parameters can affect the outcomes. Both apparent diffusion kurtosis measurement and true diffusion kurtosis are not entirely intrinsic to the tissue structures because they also depend on the MR parameters. Therefore, cautions must be taken in the quantitative interpretation of kurtosis measurements in DKI experiments.

1. Ozarslan E et al. Magn Reson Med 2003;50(5):955-965.
2. Liu C et al. Magn Reson Med 2004;51(5):924-937.
3. Jensen JH et al. Magn Reson Med 2005;53(6):1432-1440.
4. Falangola MF et al. ISMRM2007.
5. Falangola MF et al. ISMRM2007.
6. Helpert JA et al. ISMRM2007.
7. Ramani A et al. ISMRM2007.
8. Szafer A et al. Magn Reson Med 1995;33(5):697-712.
9. Sukstanskii AL et al. J Magn Reson 2002;157(1):92-105.

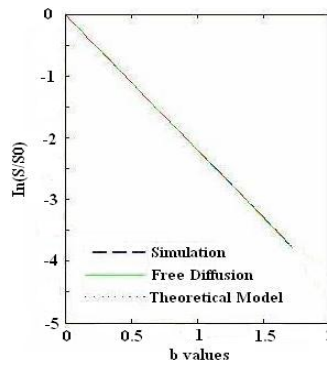


Fig. 1. Simulation of free diffusion.

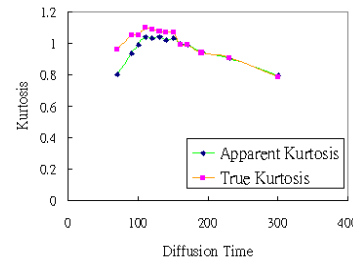


Fig. 3. Simulation of Case B for partition sizes of $13 \mu\text{m}$

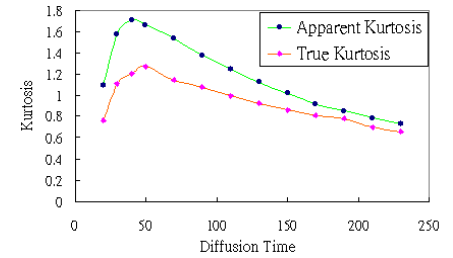


Fig. 2. Simulation of Case A for partition sizes of $7 \mu\text{m}$ and diffusion times in ms.

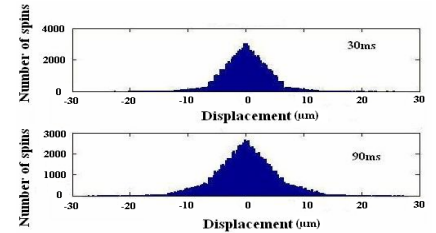


Fig. 4. Spin diffusion displacement profiles with diffusion times of 30 ms and 90 ms in simulation Case A.

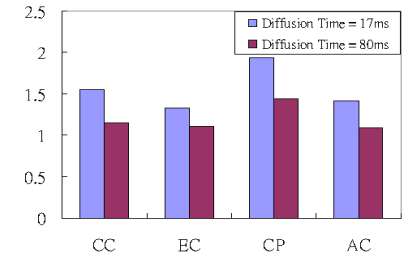


Fig. 5. Kurtosis in radial direction with different diffusion times for in vivo rat brain white matter tissues, including CC (corpus callosum), EC (external capsule), CP (cerebral peduncle), AC (anterior commissure).